



Removal of ion Cu^{2+} and Pb^{2+} using zeolite NaP1 with the silica source utilized from rice husk ash

Tran Nguyen Phuong Lan^{1*}, Nguyen Thanh Ty¹, Ly Kim Phung¹, Hong Nam Nguyen², Cao Thi Xuan Vy¹,
 Huynh Quoc Khanh¹, Tran Thi Bich Quyen¹

¹College of Engineering, Can Tho University, Can Tho, VIETNAM

²University of Science and Technology of Ha Noi, Vietnam Academy of Science and Technology, Ha Noi, VIETNAM

*Email: tnplan@ctu.edu.vn

ARTICLE INFO

Received: 15/2/2023

Accepted: 28/5/2023

Published: 30/3/2024

Keywords:

zeolite NaP1, rice husk ash,
 without aging, energy-
 saving, adsorption

ABSTRACT

Zeolite, as chemical essence, is an aluminosilicate mineral synthesized by rich-silica source, such as rice husk ash (RHA). This study focuses on the synthesis of zeolite NaP1 under a facial hydrothermal method using the silica source utilized from RHA without any -pretreatment steps. The synthesis conditions of the synthesis are achieved at the molar ratio of $8 \text{ Na}_2\text{O} : 6 \text{ SiO}_2 : 1 \text{ Al}_2\text{O}_3$, at 100°C , 8 hours, and without aging. Scanning electron microscope (SEM), dynamic light scattering (DLS), Brunauer-Emmett-Teller (BET), and X-ray diffraction (XRD) are used to determine the physical and chemical properties of the product. Adsorption results show that the optimal conditions are the initial concentration of 75 mg/L, adsorbent dose of 0.5 g/L, and contact time of 30 mins. Ion Cu^{2+} removal can reach a capacity and efficiency of 57.4 mg/g and 95.7%, respectively while Pb^{2+} adsorption can achieve a capacity and efficiency of 59.2 mg/g and 98.6%, respectively. Besides, Langmuir, Freundlich, Dubinin – Radushkevich (D-R), Temkin, Sips, and Redlich - Peterson models are also applied to describe the adsorption process.

1. Introduction

Nowadays, the rapid development of industries causing the pollution of heavy metals in the aquatic environment is more and more critical. The heavy metals such as copper, lead, arsenic, cobalt, nickel etc. used in batteries, metal plating and mining, can be of dangerous effects on plants, animals and humans [1]. There are many methods to remove heavy metals such as coagulation, membrane filtration, oxidation, biological and adsorption. Among them, the adsorption method shows the effective removal of heavy metals [2]. The choice of adsorbent is important for the adsorption process to

achieve good efficiency. Porous materials belonging to the zeolite families are well-known as potential and effective adsorbents for the removal of heavy metals [2]. Zeolite is a family of inorganic mineral materials with aluminosilicates as the main component. Its structure consists of an anionic network with porous pores; thus, zeolite can be applied for many fields, especially environmental applications [1]. The amount of RHA discharged in Mekong Delta, Vietnam is often millions of tons annually [3]. This by-product can cause the pollution owing to its small sizes, lightweight and unreasonable utilization [3]. The main component of RHA is silicon oxide (~90%), which is utilized to

<https://doi.org/10.62239/jca.2024.008>

synthesize valuable materials [4]. Therefore, the combination between heavy metals removal and the utilization of agricultural by-product for limiting environmental pollution is practical significance. In Vietnam, there are many previous studies on zeolite synthesis from minerals and by-products, and using zeolite as the adsorbent for heavy metals removal [5-8]. Zeolite NaP1 was usually synthesized over a long period ranging from one day to several days [9]. Thus, this study implements the zeolite NaP1 synthesis at a simpler process, short reaction and aging time, and obtains good adsorption capacity for heavy metal ions. The properties of zeolite NaP1 derived from RHA are also determined via SEM, DLS, BET, and XRD. Besides, the factors affecting the adsorption experiments of Cu and Pb ions are investigated. Furthermore, the experimental data are described with isotherm models to understand the adsorption process.

2. Experimental

Materials

RHA collected from Nam Tien Joint Stock Company, Tra Noc Industrial Park, Can Tho City, Vietnam was directly used for the zeolite synthesis. Chemicals included sodium hydroxide (NaOH, 96%), hydrochloric acid (HCl, 36-38%), bromothymol blue, potassium fluoride dihydrate (KF.2H₂O, 99%), sodium tetraborate decahydrate (Na₂B₄O₇.10H₂O, 99.5%), copper sulfate (CuSO₄.5H₂O, 99%), lead nitrate (Pb(NO₃)₂, 99%), potassium chloride (KCl, 99%) and potassium hydroxide (KOH, 85%) were purchased from Xilong, China. Besides, aluminum powder (Al, 99% purity) was obtained from Union Chemical Industry Company Ltd.).

Synthesis of zeolite NaP1

In this work, zeolite NaP1 is synthesized by sol-gel method, using silica source from RHA, alumina source from commercial, and NaOH as a mineralizer. The synthesis process was based on previous studies with fine modification [10]. Silica is extracted from RHA by a reaction of RHA and NaOH 5M at a ratio of 1:10 (g/mL), 90°C for 3 hours. The obtained solution mainly possesses Na₂SiO₃ in composition after removing the solid phase. NaAlO₂ solution is prepared by dissolving aluminum in NaOH solution. Then, 50 mL Na₂SiO₃ solution and 25 mL NaAlO₂ solution are placed into a round bottom flask to obtain a gel mixture and homogenized stirring step at 500 rpm, 50 °C, within 2 hours. After the reaction undergone at 100°C in 8 hours,

the solid phase is filtered and washed several times by distilled water to neutralize product pH value. A dry step at 60 °C until constant weight is required to obtain zeolite powder.

Characterization of zeolite NaP1

Products are characterized by SEM (6500F), DLS (SZ-100 Horiba), XRD (D8 Advance), and BET (Nova 1000e Quantachrome). Scherrer equation was applied as

$$D = \frac{K \cdot \lambda}{\beta \cdot \cos(\theta)} \quad (1)$$

where, D is crystallite size, K is a numerical factor frequently referred to as the crystallite-shape factor, λ is the wavelength of X-rays, β and θ are the width (full-width at half-maximum) of diffraction peak in radians and the angle, respectively.

Experiments of Cu²⁺ and Pb²⁺ removal

Zeolite NaP1 is firstly determined the surface charge by determining the point of zero charge (pH_{pzc}) method [1]. Surface charges at different pH are calculated by the pH value disparity of pre- and post-solution. Removal of Cu²⁺ and Pb²⁺ is performed at room temperature with some parameters such as the initial concentration of 10-100 mg/L, adsorbent dose of 0.25-4 g/L, and contact time of 30-150 mins. The adsorbates having pH value of 5 are chosen for all experiments and discussed in the next section. The concentrations of ion Cu²⁺ and Pb²⁺ ions in solution are detected by using Inductively Coupled Plasma (ICP, Optima 7300 DV). The adsorption result is presented as adsorption efficiency and capacity calculated by:

$$H(\%) = \frac{C_0 - C_e}{C_0} \cdot 100 \quad (2)$$

$$q_t(\text{mg/g}) = \frac{(C_0 - C_e) \cdot V}{m} \quad (3)$$

where, H (%) and q_t (mg/g) are the adsorption efficiency and capacity, respectively. C₀ and C_t (mg/L) are the concentrations of adsorbate at initial and t time (min), respectively. m (g) is a dose of zeolite and V (mL) is the volume of the solution.

Adsorption models

Adsorption models are applied to describe the adsorption process, including two-parameter (Langmuir, Freundlich, DR, and Temkin) and three-parameter (Sips and Redlich-Peterson) [11].

3. Results and discussion

Synthesis of zeolite NaP1

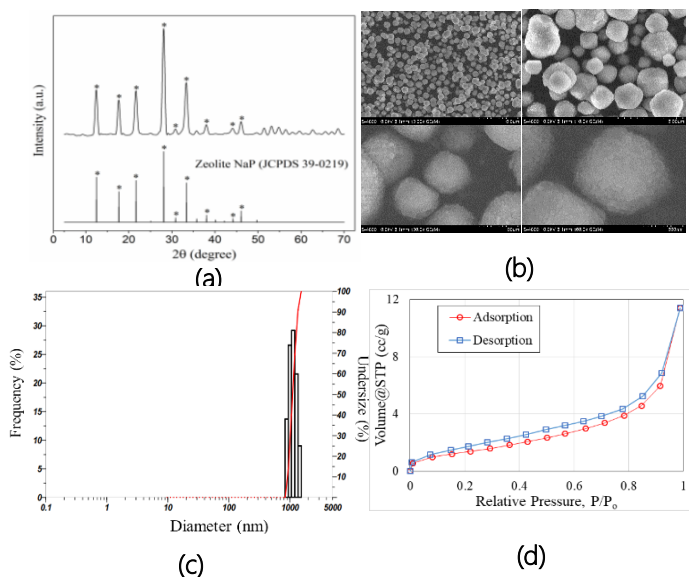


Fig 1: XRD pattern (a) and SEM images at different magnifications (b); The particle size distribution (c) and N₂ adsorption-desorption isotherms (d) of zeolite NaP1

Obtained zeolite is analyzed by XRD to examine the crystalline structure and collate with pure zeolite NaP1. XRD result in Fig 1a reveals the fine crystalline structure of zeolite with the obvious sharp peak and high intensity. In comparison of the standard peak of NaP1 (JCPDS card No. 39-0219), the synthesized zeolite possesses full of peaks fitting the standard ones, indicating the good transferring of silica into zeolite structure due to no finding of non-crystalline reagents. The crystalline size of zeolite NaP1 (16.23 nm) is identified by the Scherrer equation. To determine the crystal structure and morphology of zeolite NaP1, SEM is carried out and presented in Fig 1b at different magnifications. The SEM images suggest a well-crystal growth of the synthesized zeolite with the regular sphere shape which was similar to other study [12]. The zeolite NaP1 particles were categorized to the Gismondine group, well-known microspheres. The synthesized zeolite NaP1 is also sphere-shaped with a regular size of about 1.3 μm. Moreover, DLS result (Fig 1c) also indicates the narrow distribution and particle size of about 1.123 μm. Nano crystallites are found as well-grown on microsphere surface with the size of each crystallite size of few nanometers. This dimension agrees with the Scherrer calculation based on the XRD peak. However, the sphere particles are isolatedly dispersed but may be still aggregated. This may be due to the excess amount of an alkaline solution used, resulting in

an increased electrolyte concentration and the condensation of primary particles in the solution phase [12].

Surface texture of zeolite NaP1 is determined by N₂ adsorption/desorption and presented in Fig 1d. Zeolite NaP1 expresses a type I isotherm with no step-wise behavior. This behavior suggests the uniform pore size of material which is in agreement with the pretended pore size distribution. The observed hysteresis was assigned to the mesopore character of the material, but zeolite NaP1 does not have mesoporous structure. This phenomenon can be described owing to the smaller pore size of NaP1, compared to the kinetic diameter of nitrogen, the observed BET surface areas may not reflect the intrinsic zeolite microporosity. The surface area and pore diameter are 14 m²/g and 19.4 Å, respectively. The surface area is relatively small, similar to reported values, which could be illustrated that the structure of zeolite NaP1 only had 8-membered rings [13].

Removal of cation Cu²⁺ and Pb²⁺

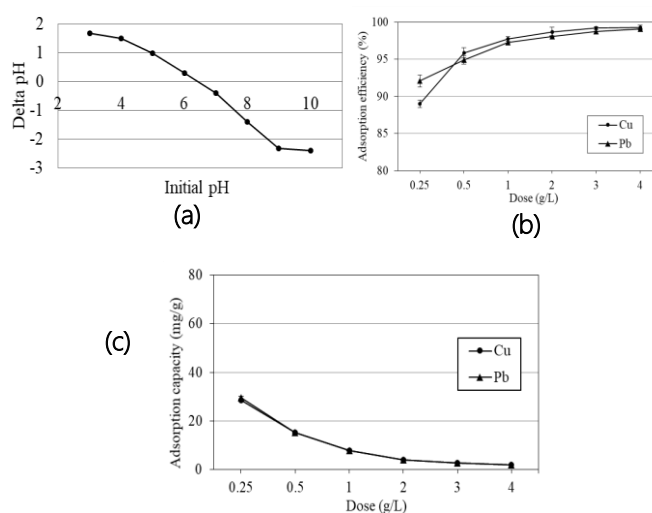
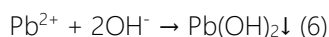
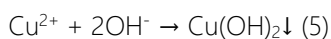


Fig 2: Plot of pH_{pzc} (a); adsorption efficiency (b) and adsorption capacity (c) at different zeolite doses (initial concentration of 20 mg/L, pH 5, 30 mins)

pH_{pzc} of zeolite NaP1 was presented at 6.41 in Fig 2a. At pH_{solution} < pH_{pzc}, the surface of zeolite NaP1 has a positive-charge, and versa. This study focuses on removal cation (Cu²⁺, Pb²⁺); thus, pH_{solution} > 6.41 should be favourable for the adsorption process. However, the high pH value of the solution causes the presence of hydroxide precipitation (Eq 5 and Eq 6), which makes the adsorption meaningless (pH 5.3 and pH 5.4 in the case of Cu²⁺ and Pb²⁺, respectively). From the experimental study, a pH value of 5 is chosen for all adsorption experiments in this work.



Effect of zeolite NaP1 dose

Adsorption experiment is carried out at the different doses of zeolite NaP1 between 0.25 and 4 mg/L. The increase of zeolite dose from 0.25 to 4 mg/L provides more total surface area as well as the number of active sites that help the adsorption process conveniently happen, so the adsorption efficiency increased from 89.0 to 99.3 %, and 92.1 to 99.1% for Cu^{2+} and Pb^{2+} adsorption, respectively (Fig 2b-c). At the dose of 1 g/L, the adsorption process may reach the equilibrium state due to the slight increase in efficiency. However, considering the adsorption capacity, a rise of zeolite dose causes a decrease in capacity. At high adsorbent dose loaded, particles trended to form aggregation because of their high surface energy which leads to decrease total surface area and the number of active sites, and to increase diffusion path length as well [14], so adsorption is obstructed. Correlating to adsorption efficiency and capacity, a 0.5 g/L adsorbent dose is selected for the subsequent evaluation.

Effect of initial concentration

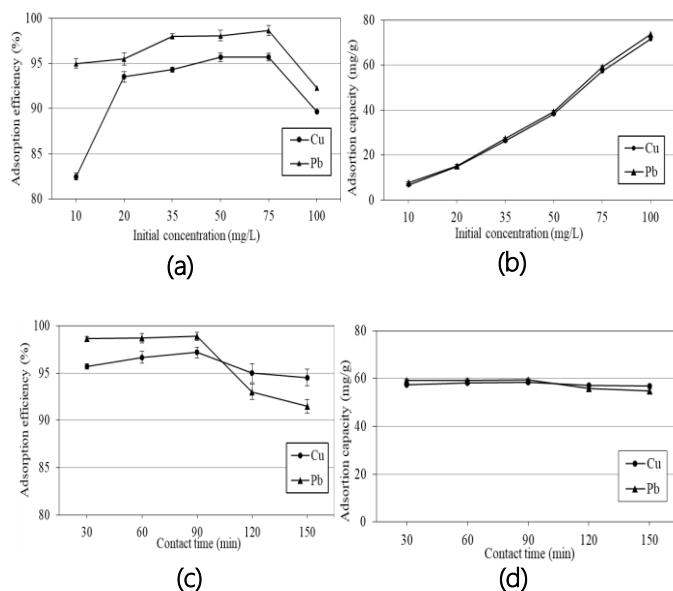


Fig 3: Adsorption efficiency (a) and adsorption capacity (b) at different initial concentrations (dose of 0.5 g/L, pH 5, 30 mins); adsorption efficiency (c) and adsorption capacity (d) at different contact time (dose of 0.5 g/L, pH 5, initial concentration 75 mg/L)

The adsorption process at different initial concentrations of cations is evaluated in Fig 3a-b. The initial

concentrations are adjusted from 10 to 100 mg/L. At period of 10-75 mg/L, the adsorption efficiency increases 82.5-95.7% (Cu^{2+} adsorption) and 95.0-98.6% (Pb^{2+} adsorption). The efficiency slightly decreases at 100 mg/L with both cations. This can be explained due to the overload of adsorbate that zeolite is not able to catch or retain. At the initial concentration of 75 mg/L, the adsorption efficiency achieved the maximum value of 95.7% (Cu^{2+}) and 98.6% (Pb^{2+}), respectively, and decreased at 100 mg/L concentration owing to the loading effect [15]. It signifies that energetically less favorable sites become involved with an increase of metal concentrations in the aqueous solution. For adsorption capacity, the increase of initial concentration results in the increased capacity of 6.6-71.7 mg/g (Cu^{2+}), 7.6-73.9 mg/g (Pb^{2+}). Based on the adsorption efficiency and capacity, the concentration of 75 mg/L is used for next study.

Effect of contact time

The Cu^{2+} and Pb^{2+} cation uptake is regarded to different mechanisms of ion-exchange processes and the adsorption process. For the ion-exchange process, ions have to move into the pores of zeolite, and then through channels of the lattice, and replace exchangeable cations, typically sodium ions in zeolite NaP1). Diffusion happens faster when the ions move through the pores and are retarded through the smaller diameter channels. For that reason, contact time is investigated from 30 to 150 mins (Fig 3c-d). The adsorption got the highest value at 90 mins and the obtained results reported that the efficiency and capacity of Cu^{2+} and Pb^{2+} are 97.2% and 58.3 mg/g, 98.9 % and 59.3 mg/g, respectively. However, the adsorption seems to reach the equilibrium state at 30 mins due to insignificant changes during the prolonged contact time. The capacity and efficiency of Cu^{2+} removal are 57.4 mg/g and 95.7%, respectively. Pb^{2+} adsorption can reveal a capacity and efficiency of 59.2 mg/g and 98.6%, respectively. At this time, the cations uptake could be mainly attributed to ion-exchange mechanism in the microporous system of zeolite [15].

Adsorption models

To describe the adsorption process, the adsorption models are presented in Table 1. Generally, experimental data fit in theoretical models but is not high reliability. For two of the adsorption process, the R^2 of the Temkin

model achieved the highest value at 0.919 for Cu²⁺ and 0.871 for Pb²⁺. The b_T factor explicitly takes into account of adsorbent–adsorbate interactions, so the adsorption process is suggested as physical adsorption (b_T<8 kJ/mol). Besides, the Langmuir model obtains the low R² value, proving that the complex of real adsorption may be an experimental error. In concentration of Q_{max} (Langmuir model) and Q_s (Sips model) seem to be equivalent that can be considered.

Table 1: The adsorption models for Cu²⁺ and Pb²⁺ adsorption

Cu ²⁺ adsorption				
Type	Model	Parameters		R ²
Two-para*	Langmuir	K _L	0.072	0.596
		Q _{max} (mg/g)	245.190	
	Freundlich	1/n _F	1.587	0.799
		K _F	9.378	
	D-R	Q _{D-R} (mg/g)	76.732	0.724
		β _{D-R} (mol ² /J ²)	0.853	
Temkin	b _T (J/mol)	0.060	0.919	
	K _T	1.080		
Three-para*	Sips	Q _S (mg/g)	268.774	0.801
		α _S	0.034	
		1/sp	1.793	
	Redlich-Peterson	K _{RP} (L/g)	14.892	0.906
		α _{RP} (L/mg)	0.576x10 ⁻⁵	
		B	0	
Pb ²⁺ adsorption				
Two-para*	Langmuir	K _L	0.118	0.400
		Q _{max} (mg/g)	392.105	
	Freundlich	1/n _F	2.492	0.606
		K _F	50.251	
	D-R	Q _{D-R} (mg/g)	161.101	0.556
		β _{D-R} (mol ² /J ²)	0.398	
Temkin	b _T (J/mol)	0.044	0.871	
	K _T	2.290		
Three-para*	Sips	Q _S (mg/g)	510.010	0.602
		α _S	0.109	
		1/sp	2.642	
	Redlich-Peterson	K _{RP} (L/g)	41.505	0.845
		α _{RP} (L/mg)	0.85x10 ⁻³	
		B	0	

* parameter

Comparison of Cu²⁺, Pb²⁺ adsorption of zeolite NaP1

Table 2: Comparison of Cu²⁺ and Pb²⁺ adsorption

Cu ²⁺ adsorption							
Type	Pre-cursor	Adsorption condition				q _e (mg/g)	Ref
		pH	C ₀ (mg/L)	Dose (g/L)	Time (min)		
NaP	fly ash	5	230	2	120	68.9	[16]
NaP	fly ash	6	100	2	180	138.1**	[17]
NaX	coal gangue	4	100	2	40	45.76	[18]
NaP1	RHA	5	75	0.5	30	57.41 245.19**	***
Pb ²⁺ adsorption							
NaP	comm*	4	200	1	45	144.70	[19]
NaX	comm*	6	10	4	1440	14.22	[20]
NaA	Fly ash	8	100	10	30	178.00	[21]
SOD	diatomite	-	1200	10	60	107.64	[8]
NaP1	RHA	5	75	0.5	30	59.21 392.11**	***

*commercial; **maximum theoretical capacity for Langmuir model; *** this work

Zeolite NaP1 is proved as the good adsorbent for the removal of both Cu²⁺ and Pb²⁺. The adsorption capacity of synthesized zeolite NaP1 is comparable to that of other kinds of zeolites (Table 2). For the case of Cu²⁺ removal, NaP1 adsorption capacity in this work is comparable to zeolite X from coal gangue and zeolite NaP from fly ash; however, the adsorption reaches the equilibrium in 30 mins and the adsorption dose used is smaller than that of other works. For the Pb²⁺ adsorption, the precursor like commercial silica was used to produce the zeolite NaP which had the high adsorption capacity (144.70 mg/g), compared to that of this work (59.21 mg/g). Moreover, a comparison between zeolite sodalite (SOD) synthesized from diatomite and zeolite NaP1 in this work revealed that the zeolite NaP1 adsorption capacity of Pb²⁺ is quite lower. It is because the zeolite NaP1 in this work is directly synthesized from RHA without any treatment, the pores of zeolite may be locked, resulted in the lower adsorption capacity of Pb²⁺ and Cu²⁺. However, the adsorption equilibrium of zeolite NaP1 reaches at shorter time (30 minutes), compared to 60 mins [9]. Generally, zeolite NaP1 is of a smaller surface area due to its structure (compared to other zeolites), but the

removal capacity of heavy metals is still satisfactory. The short contact time of 30 mins is also an interesting point of this study. Lastly, zeolite NaP1 generated from RHA performs the good adsorption capacity.

4. Conclusions

Zeolite NaP1 is successfully synthesized using a facile sol-gel method. The results have the well-crystalline of zeolite, a sphere-shape of 1.123 μm , surface area of 14 m^2/g and pore diameter of 19.4 \AA . Zeolite NaP1 is applied for removing Cu^{2+} and Pb^{2+} ions at the optimal condition: initial concentration of 75 mg/L , zeolite dose of 0.5 g/L in 30 mins. Ion Cu^{2+} removal has the capacity and efficiency of 57.4 mg/g and 95.7%, respectively while Pb^{2+} adsorption obtains a capacity and efficiency of 59.2 mg/g and 98.6%, respectively. Adsorption processes are well fitted in Temkin model and the maximum theoretical capacity reaches 245.19 mg/g (Cu^{2+} adsorption) and 392.11 mg/g (Pb^{2+} adsorption).

Acknowledgments

This research is funded by Vietnam National Foundation for Science and Technology Development (NAFOSTED) under grant number 103.02-2020.64.

References

1. S. Khan, M. Idrees, M. Bilal, *Colloids Surf. A Physicochem. Eng. Asp.* 623 (2021) 126711. <https://doi.org/10.1016/j.colsurfa.2021.126711>
2. L.R. Rad, M. Anbia, *Environ. Chem. Eng.* 95 (2021) 106088. <https://doi.org/10.1016/j.jece.2021.106088>
3. S.S. Hossain, L. Mathur, P. Roy, *J. Asian Ceram. Soc.* 64 (2018) 299-313. <https://doi.org/10.1080/21870764.2018.1539210>
4. R. Mohamed, I. Mkhallid, M. Barakat, *Arab. J. Chem.* 81 (2015) 48-53. <https://doi.org/10.1016/j.arabjc.2012.12.013>
5. D.H.L. Thanh, D.T.T. Ha, *TNU Journal of Science and Technology* 226 (2021) 93-99. <https://doi.org/10.34238/tnu-jst.4345>
6. P.T.M. Huong, N.M. Ha, *Vietnam Journal of Catalysis and Adsorption* 11 (2022) 92-97. <https://doi.org/10.51316/jca.2022.076>
7. D.Q. Huy, D.Q. Khanh, N.X. Truong, N.D. Hue, *VNU Journal of Science: Natural Sciences and Technology* 23 (2007) 160-165. <https://js.vnu.edu.vn/NST/article/view/2186>
8. N.X. Hai, N.N. Minh, L.V. Kireycheva, P.A. Hung, P.D. Pha, V.T.H. Ha, D.K. Van, *VNU Journal of Science: Natural Sciences and Technology* 27 (2011) 171-178. <https://js.vnu.edu.vn/NST/article/view/1324>
9. P. Sharma, J.S. Song, M.H. Han, C.H. Cho, *Scientific Reports* 61 (2016) 1-26. <https://doi.org/10.1038/srep22734>
10. P.L. Tran-Nguyen, K.P. Ly, L.H.V. Thanh, A.E. Angkawijaya, S.P. Santoso, N.P.D. Tran, M.L. Tsai, Y.H. Ju, *J. Taiwan Inst. Chem. Eng.* (2021) 1-8. <https://doi.org/10.1016/j.jtice.2021.05.009>
11. K.Y. Foo, B.H. Hameed, *Chem. Eng. J.* 1561 (2010) 2-10. <https://doi.org/10.1016/j.cej.2009.09.013>
12. P. Sharma, J.-g. Yeo, M.H. Han, C.H. Cho, *J. Mater. Chem.* 17 (2013) 2602-2612. <https://doi.org/10.1039/C2TA01311H>
13. I.O. Ali, S.M. El-Sheikh, T.M. Salama, M.F. Bakr, M.H. Fodial, *Sci. China Mater* 58 (2015) 621-633. <https://doi.org/10.1007/s40843-015-0075-9>
14. V.S. Raghuvanshi, U.M. Garusinghe, J. Ilavsky, W.J. Batchelor, G. Garnier, *J. Colloid Interface Sci.* 510 (2018) 190-198. <https://doi.org/10.1016/j.jcis.2017.09.064>
15. E. Erdem, N. Karapinar, R. Donat, *J. Colloid Interface Sci.* 2802 (2004) 309-314. <https://doi.org/10.1016/j.jcis.2004.08.028>
16. X. Pu, L. Yao, L. Yang, W. Jiang, X. Jiang, *J. Clean. Prod.* 265 (2020) 121822. <https://doi.org/10.1016/j.jclepro.2020.121822>
17. Y. Liu, G. Wang, L. Wang, X. Li, Q. Luo, P. Na, *Chin. J. Chem. Eng.* 272 (2019) 341-348. <https://doi.org/10.1016/j.cjche.2018.03.032>
18. X. Lu, D. Shi, J. Chen, *Environ. Earth Sci.* 76 (2017) 1-10. <https://doi.org/10.1007/s12665-017-6923-z>
19. A. Utami, S. Sugiarti, P. Sugita, *J. Rasayan J. Chem* 122 (2019) 650-658. <http://dx.doi.org/10.31788/RJC.2019.1222056>
20. P.K. Pandey, S. Sharma, S. Sambhi, *J. Environ. Chem. Eng.* 34 (2015) 2604-2610. <https://doi.org/10.1016/j.jece.2015.09.008>
21. T. Hussain, A.I. Hussain, S.A.S. Chatha, A. Ali, M. Rizwan, S. Ali, P. Ahamd, L. Wijaya, M.N. Alyemeni, *Int. J. Environ. Res. Public Health* 187 (2021) 3373. <https://doi.org/10.3390/ijerph18073373>